Published in Annals of Biomedical Engineering.
Full reference: de Vaal MH, Neville J, Scherman J, Zilla P, Litow M, Franz T. Mechanical loadings on pectoral pacemaker implants: correlation of in-line and transverse force of the pectoralis major. Ann Biomed Eng, 2010, 38(11), 3338-46

Mechanical Loadings on Pectoral Pacemaker Implants: Correlation of In-line and Transverse Force of the *Pectoralis major*

M. H. de Vaal,[1] J. Neville,[2] J. Scherman,[1] P. Zilla,[1] M. Litow,[3] T. Franz,[1]*

[1]Cardiovascular Research Unit, Chris Barnard Department of Cardiothoracic Surgery, University of Cape Town, Cape Town, South Africa

[2]Cardiac Rhythm Disease Management, Medtronic Inc, Minneapolis, MN, USA

[3]Neuromodulation Division, Medtronic Inc, Minneapolis, MN, USA

Abbreviated title: Mechanical Loadings on Pectoral Pacemaker Implants

*Send correspondence to:

Dr Thomas Franz

Cardiovascular Research Unit

Faculty of Health Sciences

University of Cape Town

Private Bag X3, 7935 Observatory, South Africa

Tel: +27-21-406 6418, Fax: +27-21-448 5935

E-mail: thomas.franz@uct.ac.za

Abstract

Background: Recently we presented a method for the assessment of *in vivo* forces on pectoral device implants motivated from technological and clinical advancements towards smaller implantable cardiac pacemakers and the altered structural demands arising from the reduced device size.

Objective: Investigation of the intra-species proportionality of in-line force and transverse reaction force of the *Pectoralis major* for the characterization of mechanical *in vivo* loadings on pectoral implants.

Methods: Two *Chacma* baboons (23.9 ± 1.2 kg) received bilaterally one chronic and one acute pectoral sub-muscular instrumented pacemaker (IPM) implant. The *Pectoralis major* muscle was electrically stimulated and resulting in-line and transverse muscle force were measured. The correlation of in-line force and transverse force of the *Pectoralis major* was investigated using linear regression analyses.

Results: The proportionality of in-line and transverse force of the *Pectoralis major* was found to be subject-specific ($R^2 = 0.17$, $p < 0.003$). Including morphometric parameters, i.e. length along line of action, width over implant and stress, in the regression analysis provided a strong intra-species correlation between in-line and transverse force ($R^2 = 0.71$, $p < 10^{-7}$).

Conclusion: The novel intra-species correlation provides a tool towards the characterization of mechanical *in vivo* loading conditions of pectoral device implants.

Keywords: Implantable pulse generator, Implantable cardioverter defibrillator, In vivo, Intra-species correlation, Linear regression analysis; Electrical stimulation, Skeletal muscle

Symbols and Abbreviations

A_{IPM}	cm^2	Total area of principal surface of IPM
A_{Si}		Surface area of force sensor cover plate
CFT	-	Constant frequency train
ETO	-	Ethylene oxide
F_{IL}	N	In-line force generated in *Pectoralis major*
F_{Si}	N	Transverse force acting on force sensor i
F_T	N	Transverse force acting on IPM
$F_{T,Rest}$	N	Transverse force on IPM with animal at rest
ICD	-	Implantable cardioverter defibrillator
IPG	-	Implantable pulse generator
IPM	-	Implantable instrumented pacemaker
L_f	mm	Muscle fibre length
$L_{f,opt}$	mm	Optimal muscle fibre length
L_m	mm	Length of *Pectoralis major* along the estimated line of action
M_B	kg	Body mass of animals
M_m	g	Mass of *Pectoralis major*
MLR	-	Multiple linear regression
N	-	Samples size
PC	-	Personal computer
PCSA	cm^2	Physiological cross-sectional area
R^2	-	Coefficient of determination
R^2_{adj}	-	Adjusted coefficient of determination
RF	-	Radio frequency
SLR	-	Single linear regression
t_m	mm	Thickness of *Pectoralis major* at the location of the IPM implant
$t_{m,cb}$	mm	Thickness of *Pectoralis major* at crossbar of the buckle force transducer
V_m	cm^3	Volume of *Pectoralis major*
V_{rest}	V	Sensor voltage at rest
$w_{m,cb}$	mm	Width of *Pectoralis major* section at crossbar of the buckle force transducer
$w_{m,IPM}$	mm	Width of *Pectoralis major* over the IPM implant
ΔF_T	N	Difference in transverse force
ρ_m	g/cm^3	Material density of *Pectoralis major*
σ_m	N/mm^2	Stress in *Pectoralis major*

1 Introduction

Implantable pulse generators (IPG; "pacemakers") and cardioverter defibrillators (ICD) have been used extensively for the therapy of cardiac arrhythmias. These devices significantly increased the clinical benefits compared to purely pharmacological treatment[1] and reduce the mortality in high-risk patient populations[2].

Technological advances in recent years have offered the potential to reduce the dimensions of implantable pacemakers[2-4]. Together with clinical advances, this development increases the feasibility of implantable pacemaker technology for use in younger patients[3,5,6] which are generally more active than the traditional target group of elderly patients. Smaller structures and elevated levels of activity translate into increased mechanical demands on the implants and smaller margins for structural reliability. The detailed knowledge of the mechanical *in vivo* use conditions of implantable pacemakers becomes more important for the device design in order to ensure structural integrity and device reliability.

Cardiac pacemakers are implanted in retro mammary, abdominal and pectoral positions. The retro mammary position is preferred in female patients, mainly for cosmetic considerations[7], whereas the abdominal region is mostly used when the physical conditions of the pectoral region are inappropriate. Pectoral implants have been shown to cause fewer complications compared to devices in the abdominal position[8]. Consequently, the pectoral region has been utilized more frequently as implant site. Here, the housing is placed in a tissue pocket either sub-cutaneously, resting on the *Pectoralis major*, or sub/intra-muscularly between the *Pectoralis major* and the *Pectoralis minor* and rib cage, respectively[9].

The mechanics and reliability of pacemaker leads has been studied extensively[8,10-13]. In contrast, the mechanical *in vivo* conditions of the pacemaker structure have not received much attention in the past. Therefore, we recently studied the feasibility of a pre-clinical measurement system for *in vivo* mechanical loading conditions of implanted pacemakers[14]. The key component of the system is an instrumented implantable pacemaker which measures the contact forces on the implant from the surrounding anatomical structures such as pectoral muscles and ribs. For sub-muscular pectoral implants, the *Pectoralis major* is the principle muscle creating a compressive mechanical loading, on the pacemaker housing, that is orientated predominantly transversely to the line of action of the muscle.

The focus of the current study is the investigation of a relationship between the force of the *Pectoralis major* muscle in line of its action, i.e. in-line force, and the transverse force

exerted on a pacemaker structure implanted in the sub-muscular position. The in-line force of the *Pectoralis major* muscle can be assessed with surface-based measurement techniques such as electro myography. A correlation between in-line and transverse force of the *Pectoralis major* may as such allow for the non-invasive characterization of *in vivo* mechanical conditions of pacemaker implants in volunteers compared to invasive measurement of the *in vivo* mechanical loadings on pacemakers with the recently developed system.

2 Materials and Methods

2.1 Measurement Systems

Measurement of in-line muscle force

A custom-made stainless steel buckle transducer with closed rectangular frame (66 x 100 mm, 4 x 4 mm cross-section), removable cross bar (semi-circular cross section: R = 2 mm) and two linear foil strain gauges (EA-DY-125BT-350, Vishay Micro Measurements Group, Malvern, PA) (Fig. 1) were utilized for the measurement of the in-line force associated with muscle contraction. The strain gauges were operated with a custom-built Wheatstone half-bridge amplifier connected to a PC Laptop (Dell Latitude M65, Dell, Round Rock, TX). Data acquisition was performed using a custom code in LABVIEW (National Instruments Corp, Austin, TX).

Measurement of transverse muscle force

A wireless *in vivo* measurement system described in detail previously[14,15] was used for this study. In brief, the system comprised an implantable instrumented pacemaker (IPM) and a radio-frequency (RF) control and data acquisition system. The IPM was a medical grade epoxy cast (dimensions: 64 x 61 x 11 mm, volume: 29 cm^3, see Fig. 2), resembling a typical commercial pacemaker housing, containing six custom manufactured contact force sensors (Tekscan, Boston, MA) with Titanium cover plates, a three-axis accelerometer (Freescale Semiconductor, Tempe, AZ), RF transceiver, micro-controller, real-time clock and high energy lithium battery. The RF data transmission system comprised a custom built RF transceiver and a PC laptop (Dell Latitude, Dell, Round Rock, TX) linked through a serial RS232 connection. A custom software code (LABVIEW, National Instruments Corp, Austin, TX) was used to control the IPM circuitry and the data acquisition. The force sensors of each

IPM were preconditioned for 4 weeks with a mild static compression load, relative humidity (100%) and temperature (37°C) simulating *in vivo* conditions at rest. Calibration of the force sensors[15] was performed regularly repeatedly throughout the precondition procedure, prior to implantation and after explantation to monitor the sensor sensitivity. The calibrations were performed on an Instron 5544 universal testing machine with a 500 N load cell (Instron Corp, Norwood, MA) using a custom-build fixture to hold the IPM. A compressive force (0 to 44.5 N, cross-head speed: 0.254 mm/min) was applied with a stainless steel pin (diameter 9.5mm, flat end) to each sensor individually, while capturing data of the force sensor with the RF acquisition system. The data recorded with the IPM and the Instron 5544 were analyzed, and calibration curves were generated using a custom code in MATLAB (MathWorks Inc, Natick, MA)[14]. Fifth-degree polynomials fitted to the experimental calibration curves were facilitated for the voltage-force conversion. The calibration performed within 4 hours after IPM explantation served as reference for the data analysis. The IPM devices were sterilized (ETO, 55°C, 60% relative humidity, 12 hours) within 24 hours prior to implantation.

Raw voltage data of the force sensors was median filtered (n = 7) to reduce noise levels and converted to force data employing a custom algorithm in MATLAB (MathWorks Inc, Natick, MA)[15]. Assuming an equal distribution of the compressive force acting in the normal direction on the in-plane surface of the IPM, the total transverse force F_T was calculated from the individual forces recorded with the six sensors, F_{Si}, the surface areas of the sensor cover plates, A_{Si} and the total area of the IPM in-plane surface A_{IPM} to the sum of the areas of the sensor cover plates:

$$F_T = \frac{A_{IPM}}{\sum_{i=1}^{6} A_{Si}} \sum_{i=1}^{6} F_{Si} \,. \quad (1)$$

2.2 In vivo Experiments

This study was approved by the research ethics committee of the University of Cape Town.

Implantation

Under full anesthesia, two senescent *Chacma* baboons (implant mass: 23.9 ± 1.2 kg) received one IPM unilaterally in the upper pectoral region (left side: one animal, right side: one animal). The IPM was implanted in the sub-muscularly position with the force-sensing surface facing outwards and secured in place with two sutures. The procedures were performed using standard surgical techniques for the implantation of cardiac pacemakers. Ten weeks after implantation, with the IPM implants having obtained fibrous encapsulation, the

Pectoralis major muscle was exposed by removing overlying skin with the animals under full anesthesia. The muscle was isolated from surrounding soft tissue. To attach the buckle force transducer, two incisions were made in the fiber direction of the muscle extending from the IPM implant towards the insertion of the muscle. The frame of the buckle transducer was positioned over the muscle section between the incisions and secured in place with the crossbar (Fig. 3). Pre-gelled disposable adhesive surface electrodes (Model 9013S0211, Medtronic Inc, Minneapolis, MN) were attached to the exposed *Pectoralis major* muscle near its origin and insertion for electrical stimulation. At the same occasion, identical procedures were performed on the alternate pectoral side without chronic IPM implant for both animals. The alternate pectoral side received, however, an acute IPM implant for the force measurement procedure.

Electrical Stimulation and Measurement of Forces

Constant frequency train (CFT) stimulation of the *Pectoralis major* was performed using a PULSAR 6bp bipolar stimulator (FHC Inc, Bowdoinham, ME) and pre-gelled surface electrodes (see "Implantation"). The exposed and isolated muscle received trains of electrical current of constant, discrete amplitude of 3, 5, 7, 9, 11, 15, 17, 21, 23, 27, 31, 33, and 35 mA in one of two pre-determined randomized order. Each train comprised 2000 pulses with pulse duration of 53 μs and pulse interval of 203 μs. The selected amplitude range of the current and the randomization aimed at reaching maximum activation and minimizing fatigue, respectively, of the muscle. The arm of the baboon was constrained in the anatomical position whereas the shoulder complex was left to move freely, which led to the generation of a concentric (non-isometric) contraction of the muscle. The contractile force F_{IL} developed in the stimulated muscle was measured with the buckle force transducer. The transverse force F_T of the contracting muscle was recorded with the implanted IPM and the wire-less measurement system. The maximum forces F_T and F_{IL} were identified for each stimulation train.

Morphometric Measurements

Post-mortem, the following dimensions of the *Pectoralis major* were measured using a ruler and caliper, respectively: the length along the estimated line of action (L_m), thickness and width at the crossbar of the buckle force transducer ($t_{m,cb}$, $w_{m,cb}$), and width over the IPM implant ($w_{m,IPM}$). After excision, the mass (M_m) and volume (V_m) of the muscle were recorded using a scale and a fluid displacement method, respectively.

2.3 Correlation of In-line Force and Transverse Force of the Pectoralis major

Simple and multiple linear regression (SLR and MLR) analyses were performed to evaluate the relationship between the in-line force F_{IL} and the transverse force F_T of the *Pectoralis major* muscle and to identify significant parameters of this relationship. The transverse force F_T and the relative transverse force $\Delta F_T = F_T - F_{T,Rest}$ were alternatively defined as response. The in-line force of the *Pectoralis major*, F_{IL}, and the measured morphometric muscle parameters, L_m, $t_{m,cb}$, $w_{m,cb}$, $w_{m,IPM}$, M_m, and V_m, were regarded as input parameters (regressors). Although not measured directly, two additional regressors were considered; the physiological cross-sectional area (PCSA)[16] defined as

$$PCSA = \frac{V_m}{L_m} \cdot \frac{L_f}{L_{f,opt}} \tag{2}$$

where L_f and $L_{f,opt}$ were the muscle fiber length and optimal muscle fiber length, respectively, and the stress σ_m in the *Pectoralis major*

$$\sigma_m = \frac{F_{IL}}{PCSA}\,. \tag{3}$$

The PCSA was included as it scaled proportionately with, and as such related to, the maximum isometric force of a muscle, $F_{IL,opt}$, at optimal muscle fiber length, $L_{f,opt}$. The muscle fiber length and the optimal muscle fiber length was assumed to be similar, and the ratio $L_f/L_{f,opt}$ to be unity, for all *Pectoralis major* muscles of the two animals. The muscle stress σ_m was considered in the analyses since it was a unique interpretable parameter combining force and a morphometric parameter of the muscle.

To account for the increase of the degree of freedom associated with the addition of regressors in an MLR analysis, an adjusted coefficient of determination, R^2_{adj}[17] was used. R^2_{adj} indicates a genuine improvement in correlation as compared to an apparent improvement of a correlation associated with an increased value for the non-adjusted coefficient of determination, R^2, with an increasing number of regressors.

2.4 Statistical Analysis

Continuous data was expressed as individual figures and mean ± standard deviation, respectively. Categorical data was expressed as median. The significance of simple and multiple linear regression analyses (Statistica 8, Statsoft, Tulsa, OK, USA) were assessed using the coefficient of determination, R^2, and the adjusted coefficient of determination, R^2_{adj}, where applicable. Correlation results obtained from multiple regression analyses were

evaluated for model misspecification by observing the distribution of residuals, as well as the correlation between regression obtained coefficients. The significance of a correlation was evaluated by calculating the non-directional probability of the correlation coefficient, R, using t-statistics with $t = R/\sqrt{(1-R^2)/(N-2)}$ where N is the sample size (Statistica 8, Statsoft, Tulsa, OK, USA). Statistical significance was assumed for p values smaller than 0.05.

The approach of forward-stepwise multiple linear regression involves (1) identifying an initial model, (2) iteratively "stepping," that is, repeatedly altering the model at the previous step by adding or removing a predictor variable in accordance with the "stepping criteria," and (3) terminating the search when stepping is no longer possible, or when a specified maximum number of steps has been reached. The forward-stepwise method employs a combination of forward entry and backward removal methods. At the first step, the procedure of forward entry is performed. At any subsequent step where two or more effects have been selected for entry into the model, forward entry is performed if possible, and backward removal is performed if possible, until neither procedure can be performed and stepping is terminated. In forward entry, the effect with the largest value on the entry statistic is entered into the model whereas the effect with the smallest value on the removal statistic is removed from the model in backward removal.[18]

3 Results

3.1 Morphometric Parameters of the Pectoralis major

The *Pectoralis major* muscles exhibited an average mass of 131.8 ± 37.4 g and volume of 118.8 ± 34.7 cm^3, resulting in a material density of 1.115 ± 0.055 g/cm^3. The individual values for these parameters as well as for the muscle dimensions and PCSA are summarized in Table 1.

3.2 Forces during Electrical Stimulation

The in-line forces F_{IL} of the *Pectoralis major* recorded during each set of electrical stimulations for all four experiments are illustrated in Fig. 4. The in-line force F_{IL} varied in the ranges of 0.9 – 60.9 N (447C) and 3.6 - 85.0 N (449C) for the chronic IPM implants whereas the force ranges were larger for the acute implants with 30.9 – 184.3 N (447A) and 1.1 – 155.1 N (449A). The maximum force was observed for the maximum level of

stimulation current for two implants, 449C and 449A, only. For the implants 447C and 447A, the maximum force activation was obtained at sub-maximal current levels prior to maximum stimulation.

The transverse force F_T of the *Pectoralis major* associated with the in-line force F_{IL} during electrical stimulation is illustrated in Fig. 5 for all four implants. The transverse force was measured in the following ranges: 5.4 – 9.2 N (447C), 9.2 – 41.7 N (449A), 9.5 – 55.8 (447A) and 14.3 – 90.7 N (449C). While there was a distinct difference with regards to the maximum F_{IL} between chronic (low F_{IL}) and acute implants (high F_{IL}), this was not the case for the transverse force.

3.3 Correlation of In-line Force F_{IL} and Transverse Force F_T

Subject-specific Correlation

SLR analyses of the corresponding F_T - F_{IL} data indicated significant correlation ($p < 0.05$) between the transverse force and in-line force for each *Pectoralis major* muscle and IPM implant, respectively. The subject-specific linear regression, indicated by the trend lines in Fig. 5, yielded the following relationships and associated coefficients of determination; **447C**: $F_T = 0.06\ F_{IL} + 5.24$, $R^2 = 0.80$; **449C**: $F_T = 0.99\ F_{IL} + 8.63$, $R^2 = 0.97$; **447A**: $F_T = 0.17\ F_{IL} + 5.03$, $R^2 = 0.56$; and **449A**: $F_T = 0.23\ F_{IL} + 7.47$, $R^2 = 0.96$.

Generalized Correlation

The generalized intra-species correlation was evaluated by performing SLR and MLR analyses on the entire data set of F_T and F_{IL} (n=51) from all four experiments (447C, 447A, 449C and 449A). The single linear regression analysis with F_T and ΔF_T, respectively, as response and F_{IL} as single regressor indicated poor correlation with R^2 of 0.17 and 0.21 (Table 2, cases A and D).

Employing a forward-stepwise MLR approach, the strongest correlations were obtained when all considered regressors were included in the analysis (Table 2, cases C and F). The strongest correlation with R^2 and R^2_{adj} of 0.71 and 0.68, respectively, was indicated for the response F_T (case C) and yielded the following regression equation:

$$F_T = -1055.78 - 0.24\ F_{IL} + 3.24\ L_m + 5.95\ w_{m,IPM} + 434.62\ \sigma_m \quad (4)$$

Figure 6 illustrates the relationship between the predicted, using Eq. (4), and the measured values of F_T.

4 Discussion

The purpose of this study was to investigate the relationship between the in-line force and transverse force of the *Pectoralis major* muscle to gain knowledge towards the mechanical loading environment of cardiac pacemakers, and other medical devices, typically implanted sub-muscularly in the pectoral region. By combining electrical stimulation of the *Pectoralis major*, the measurement of this muscle's in-line force with a buckle transducer and a newly developed method to measure *in vivo* the transverse force of the *Pectoralis major*[14], both a subject-specific proportionality and an intra-specific correlation between in-line force and transverse force of the *Pectoralis major* could be established.

The study was conducted in the non-human primate model (Chacma baboon) since the baboon was assumed to be most suitable model for these investigations. One essential, and unique, feature, compared to other laboratory animals, was the presence of a clavicle that enabled movements of the upper limb similar to humans[19]. Furthermore, the pectoral implantation site of the IPM in the baboons compared very well with those of humans. The material density of the *Pectoralis major* muscle of 1.115 ± 0.055 g/cm^3 of this study, determined on freshly excised tissue, compared well with previously reported values for mammalian muscle tissue of 1.112 ± 0.006 g/cm^3, measured on muscle tissue after fixation in 4% formaldehyde[20].

Through graded contractions, the experiments revealed the subject-specific proportionality between the in-line force F_{IL} and the transverse force F_T both for the chronic and acute IPM implants (see Fig. 5). The ratio F_T/F_{IL} varied between 0.06 and 0.99 with F_T ranging between 5.03 N and 8.6 N for F_{IL} = 0 N. The subject-specificity of this relationship was confirmed by results of the generalized correlation which indicated a poor correlation between F_{IL} and F_T (R^2 = 0.17) when data of all implants was included (case A, Table 2).

A significant intra-species correlation was found between transverse force F_T and in-line force (R^2 = 0.71, $p < 0.001$) of the *Pectoralis major* with additional regressors of the stress σ_m in the *Pectoralis major*, originating from the in-line force F_{IL}, the length L_m of the muscle and the width of the muscle over the IPM, $w_{m,IPM}$. Although F_{IL} marginally failed to reach significance (p = 0.055), it was included in the regression equation since it (a) constituted one of the two principal parameters of interest of this study, F_T and F_{IL}, and (b) was measured experimentally, unlike σ_m which was a derived parameter (see Eq. 3).

The strength of the intra-species correlation was not affected by the estimation of the parameters $L_f/L_{f,opt}$ and cos θ, both considered to be unity for all subjects. These assumptions were deemed reasonable since the animals used in the study were of the same species, same gender and similar body masses. The variation of the fiber length, L_f, and the optimal fiber length, $L_{f,opt}$, of a muscle has been reported to remain minimal when scaling these parameters with respect to body mass in different test subjects of the same species[21]. While the uncertainty of these parameters may have affected the predicted magnitude of F_T, the specific formulation of the linear regression relationships ensured that the correlation of response and regressors was not affected[17].

For the chronic implants (447C, 449C), the maximum in-line force $F_{IL,max}$ was significantly lower than that of the acute implants (447A, 449A): 73.0 ± 17.0 N vs. 169.7 ± 20.6 N, p = 0.036. Differences of the morphometric parameters of the *Pectoralis major*, such as mass M_m, volume V_m and physiological cross-sectional area PCSA, could however not be established. It is suggested that the strength of the intra-species F_T-F_{IL} correlation will improve beyond the value of R^2 = 0.71 obtained when the analysis is limited at chronic implants only. Due to the feasibility character of the presented study with two animals and two implants per group (chronic and acute), this separation was not practical. Despite the fact that the significant difference between chronic and acute implants observed for $F_{IL,max}$ did not extend to the maximum transverse force $F_{T,max}$, these results are seen as a strong indication for the benefit of this *in vivo* study, and presented method, over cadaver studies; namely the ability to capture the effect of fibrous encapsulation on the *in vivo* biomechanics of the implant.

It remained uncertain whether maximum levels of F_{IL} and F_T, respectively, were reached during the electrical stimulation experiments. The maximum electrical current did not always yield the maximum magnitude of the in-line force F_{IL} (Fig. 4). Accelerated muscle fatigue due to the CFT stimulation compared to variable frequency train (VFT) stimulation[22] may have played a role. However, the CFT stimulation was chosen in this study as this method is used in most current systems for functional electrical stimulation[23] and generally provides a more physiological stimulation pattern. A further factor may have been potential differences in the maximum levels of F_{IL} due to concentric, isometric and eccentric contractions[24].

The definition of the PCSA (see Eq. 2)[16] used in this study did not account for the pennation angle θ of the muscle fibers as compared to a more comprehensive formulation of the PCSA that considers this parameter[25]. This simplification was based on the assumption that the

pennation angle of the *Pectoralis major* muscle did neither differ between the bilateral sides of each subject nor between subjects of this study.

5 Conclusions

In this study, an intra-species correlation between in-line force and transverse reaction force of the *Pectoralis major* muscle was developed based on experimental measurements in the baboon model. With the motivation for this study to quantify *in vivo* forces on pacemaker devices implanted sub-muscularly in the pectoral region, the established intra-species relationship may offer potential towards gaining new insights in biomechanics of such implants in patients. One requirement is a more detailed assessment of the proposed relationship with regards to the distinctiveness and the precision of individual parameters and the robustness of the relationship based on a larger subject cohort. Furthermore, inter-species differences will need to be considered in an extended and more comprehensive relationship.

Acknowledgements

The authors thank Professor Stephen Beningfield, Patronella Samuels, Sharon Heyne and Nazlea Behardien-Peters of the Department of Radiology, University of Cape Town, for MRI and CT imaging.

Conflict of Interest Statement

The authors confirm that they do not have conflicts of interest in connection with the work and data are presented in this paper.

References

1. Cleland, J. G. F., J.-C. Daubert, E. Erdmann, N. Freemantle, D. Gras, L. Kappenberger and L. Tavazzi. The effect of cardiac resynchronization on morbidity and mortality in heart failure. N. Engl. J. Med. 352:1539-1549, 2005.
2. Maisel, W. H., M. Moynahan, B. D. Zuckerman, T. P. Gross, O. H. Tovar, D.-B. Tillman and D. B. Schultz. Pacemaker and icd generator malfunctions: Analysis of food and drug administration annual reports. J. Am. Med. Assoc. 295:1901-1906, 2006.

3. Furman, S. The future of the pacemaker. Pacing Clin. Electrophysiol. 25:1-2, 2002.
4. Shmulewitz, A., R. Langer and J. Patton. Convergence in biomedical technology. Nat. Biotechnol. 24:277-280, 2006.
5. Antretter, H., J. Colvin, U. Schweigmann, H. Hangler, D. Hofer, K. Dunst, J. Margreiter and G. Laufer. Special problems of pacing in children. Indian Pacing Electrophysiol. J. 3:23-33, 2003.
6. Friedman, R. A. Pacemakers in children: Medical and surgical aspects. Tex. Heart Inst. J. 19:178-184, 1992.
7. Kenny, T. The Nuts and Bolts of Cardiac Pacing. Malden: Blackwell Futura, 2005, 162 pp.
8. Kron, J., J. Herre, E. G. Renfroe, C. Rizo-Patron, M. Raitt, B. Halperin, M. Gold, B. Goldner, M. Wathen, B. Wilkoff, A. Olarte and Q. Yao. Lead- and device-related complications in the antiarrhythmics versus implantable defibrillators trial. Am. Heart J. 141:92-98, 2001.
9. Kistler, P. M., N. Eizenberg, S. P. Fynn and H. G. Mond. The subpectoral pacemaker implant: It isnt what it seems. Pacing Clin. Electrophysiol. 27:361-364, 2004.
10. Baxter, W. W. and A. D. McCulloch. In vivo finite element model-based image analysis of pacemaker lead mechanics. Med. Image Anal. 5:255-270, 2001.
11. Fortescue, E. B., C. I. Berul, F. Cecchin, E. P. Walsh, J. K. Triedman and M. E. Alexander. Patient, procedural, and hardware factors associated with pacemaker lead failures in pediatrics and congenital heart disease. Heart Rhythm 1:150-159, 2004.
12. Hauser, R. G., D. L. Hayes, L. M. Kallinen, D. S. Cannom, A. E. Epstein, A. K. Almquist, S. L. Song, G. F. O. Tyers, S. C. Vlay and M. Irwin. Clinical experience with pacemaker pulse generators and transvenous leads: An 8-year prospective multicenter study. Heart Rhythm 4:154-160, 2007.
13. Mattke, S., D. Muller, A. Markewitz, H. Kaulbach, M. Schmockel, U. Drwarth, E. Hoffmann and G. Steinbeck. Failures of epicardial and transvenous leads for implantable cardioverter defibrillators. Am. Heart J. 130:1040-1044, 1995.
14. de Vaal, M. H., J. Neville, J. Scherman, P. Zilla, M. Litow and T. Franz. The in vivo assessment of mechanical loadings on pectoral pacemaker implants. J. Biomech. DOI: 10.1016/j.jbiomech.2010.02.028, 2010.
15. de Vaal, M. H. *In vivo* mechanical loading conditions of pectorally implanted cardiac pacemakers: Feasibility of a force measurement system and concept of an animal-

human transfer function [MSc thesis]. Cape Town: Chris Barnard Department of Cardiothoracic Surgery, University of Cape Town; 2009.

16. Holzbaur, K. R. S., W. M. Murray, G. E. Gold and S. L. Delp. Upper limb muscle volumes in adult subjects. J. Biomech. 40:742-749, 2007.
17. Vining, G. G. Statistical methods for engineers. London: Brooks/Cole, 1998, 479 pp.
18. Hill, T. and P. Lewicki. Statistics Methods and Applications. Tulsa, OK: StatSoft, 2007.
19. Voisin, J. L. Clavivle, a neglected bone: Morphology and relation to arm movements and shoulder architecture in primates. Anat. Rec. 288A:944-953, 2006.
20. Ward, S. R. and R. L. Lieber. Density and hydration of fresh and fixed human skeletal muscle. J. Biomech. 38:2317-2320, 2005.
21. Eng, C. M., L. H. Smallwood, M. P. Rainiero, M. Lahey, S. R. Ward and R. L. Lieber. Scaling of muscle architecture and fiber types in the rat hindlimb. J. Exp. Biol. 211:2336-2345, 2008.
22. Binder-Macleod, S. A., S. C. K. Lee, D. W. Russ and L. J. Kucharski. Effects of activation pattern on human skeletal muscle fatigue. Muscle Nerve 21:1145-1152, 1998.
23. Ding, J., S. C. K. Lee, T. E. Johnston, A. S. Wexler, W. B. Scott and S. A. Binder-Macleod. Mathematical model that predicts isometric muscle forces for individuals with spinal cord injuries. Muscle Nerve 31:702-712, 2005.
24. Pasquet, B., A. Carpentier, J. Duchateau and K. Hainaut. Muscle fatigue during concentric and eccentric contractions. Muscle Nerve 23:1727-1735, 2000.
25. Powell, P. L., R. R. Roy, P. Kanim, M. A. Bello and V. R. Edgerton. Predictability of skeletal muscle tension from architectural determinations in guinea pig hindlimbs. J. Appl. Physiol. 57:1715-1721, 1984.

Tables

Table 1. Body mass of the animals and morphometric parameters of the *Pectoralis major* muscles.

Parameter	**Implant No**				**Overall**
	447C	**447A**	**449C**	**449A**	
M_B [kg]	24.7		23.0		23.9 ± 1.2
M_m [g]	82	154	125	166	131.8 ± 37.4
V_m [cm^3]	70	135	120	150	118.8 ± 34.7
ρ_m [g/cm^3]	1.171	1.141	1.042	1.107	1.115 ± 0.055
$t_{m,cb}$ [mm]	5	4	4	6.5	4.9 ± 1.2
$w_{m,cb}$ [mm]	42.5	60	47.5	50	50.0 ± 7.4
$w_{m,IPM}$ [mm]	92.5	95	90	80	89.4 ± 6.6
L_m [mm]	150	150	170	180	163 ± 15
PCSA* [cm^2]	7.7	14.8	11.6	13.7	12.0 ± 3.1

*with assumption of $L_f/L_{f,opt} = 1$

Table 2: Significances of individual regressors, normal and adjusted coefficients of determination and correlation significance obtained in linear regression analyses for various combinations of experimental parameters.

Case	**Response**	**Individual significance (p) of correlation for regressors**									**Correlation results**		
		F_{IL}	$t_{m,cb}$	L_m	$w_{m,IPM}$	$w_{m,cb}$	V_m	M_m	PCSA	σ_m	R^2	R^2_{adj}	p
A	F_T	0.0028									0.17	0.15	0.0028
B	F_T	$< 10^{-7}$	n	$< 10^{-7}$	$< 10^{-7}$	0.0014	n	n			0.69	0.66	$< 10^{-7}$
C	F_T	0.0545	n	$< 10^{-7}$	$< 10^{-7}$	n	n	n	n	0.0004	0.71	0.68	$< 10^{-7}$
D	ΔF_T	0.0007									0.21	0.19	0.0007
E	ΔF_T	$< 10^{-7}$	n	s	$< 10^{-7}$	0.0010	n	n			0.63	0.60	$< 10^{-7}$
F	ΔF_T	n	0.0371	0.0076	0.0175	n	n	n	n	$< 10^{-7}$	0.65	0.62	$< 10^{-7}$

n Regressor used but no correlation indicated

Figures

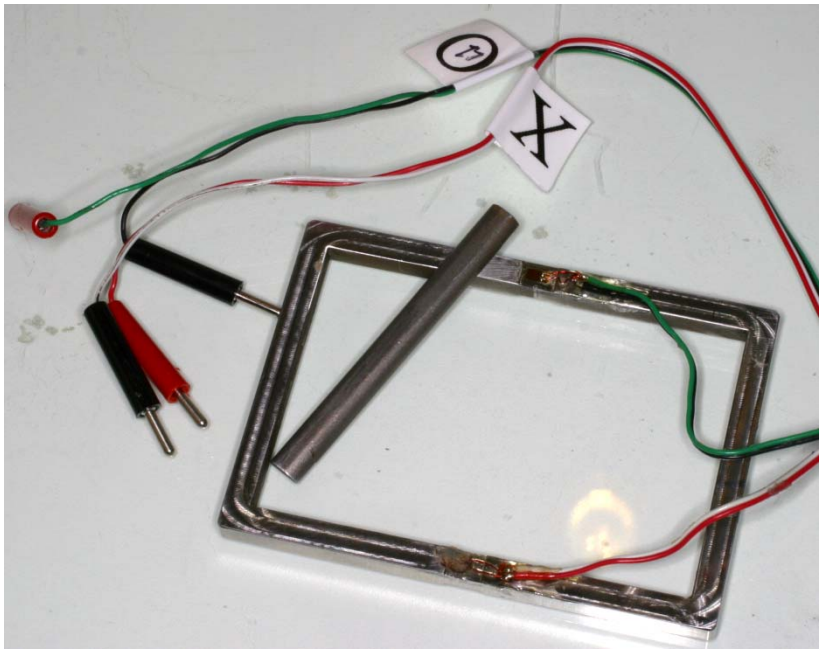

Figure 1. Buckle force transducer with foil strain gauges for the measurement of in-line force of the *Pectoralis major*.

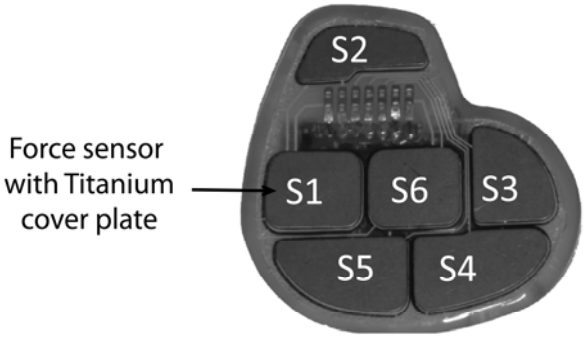

Figure 2. Photograph of instrumented pacemaker showing the Titanium plates covering the six contact forces sensors (S1 to S6).

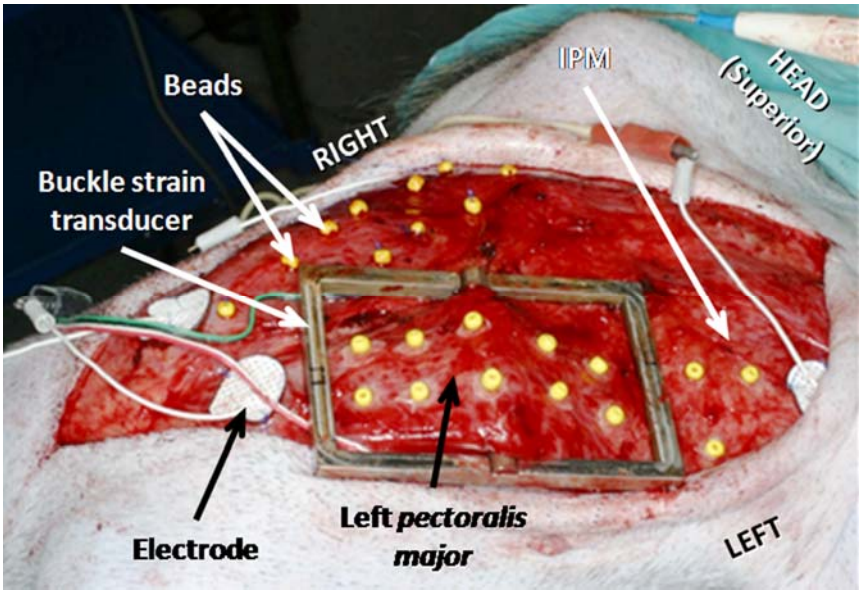

Figure 3. Photograph showing the exposed *Pectoralis major* muscle with attached buckle force transducer and electrodes for electrical stimulation experiments. (The beads attached to the muscle were used for an unrelated study.)

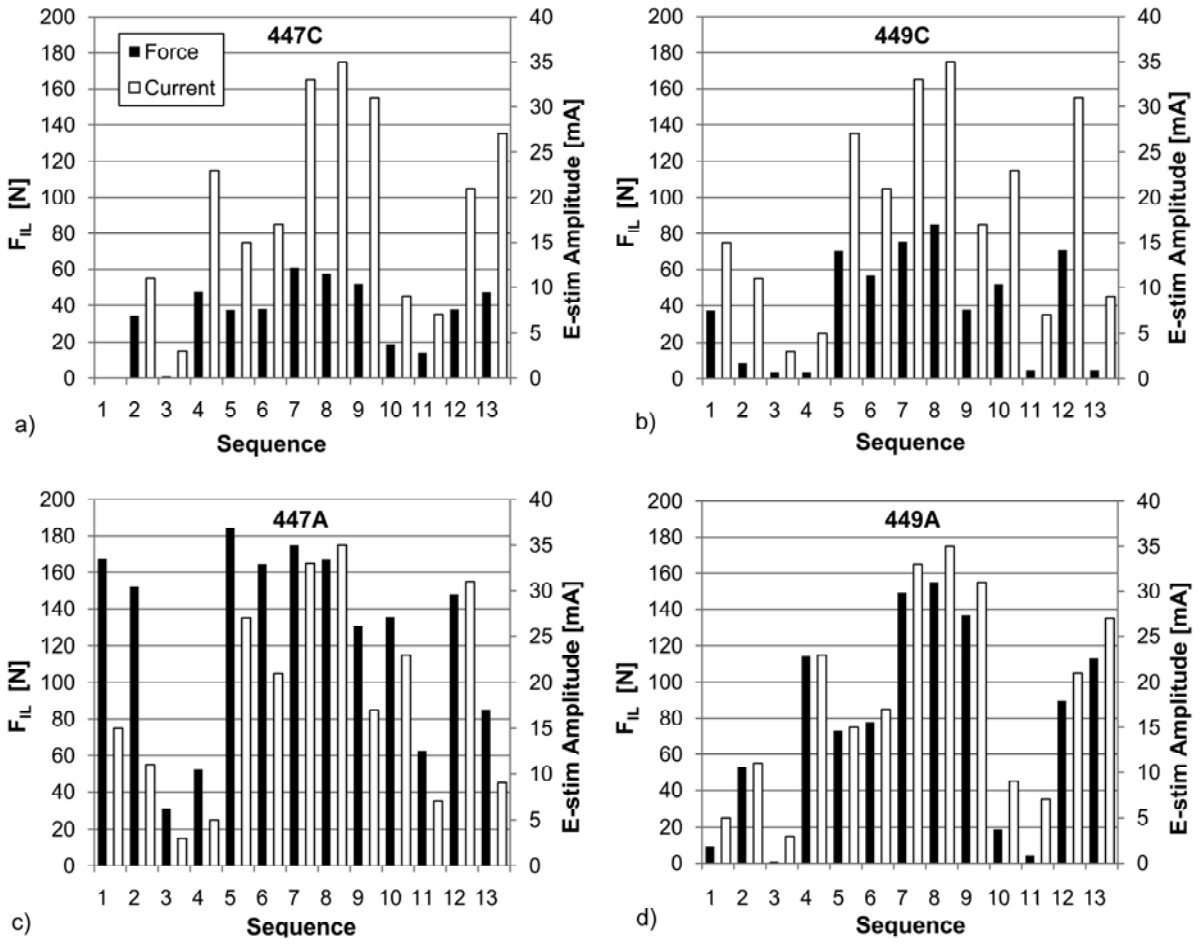

Figure 4. The in-line muscle force F_{IL} (filled bars) and associated amplitude of electrical current (open bars) during the 13 pulse trains of the electrical stimulation for each experiment: a) chronic implant 447C, b) chronic implant 449C, c) acute implant 447A and d) acute implant 449A. Note: For experiment 447C, the first data pair is not included due to a malfunction of the in-line force measurement during the stimulation with current amplitude of 5mA.

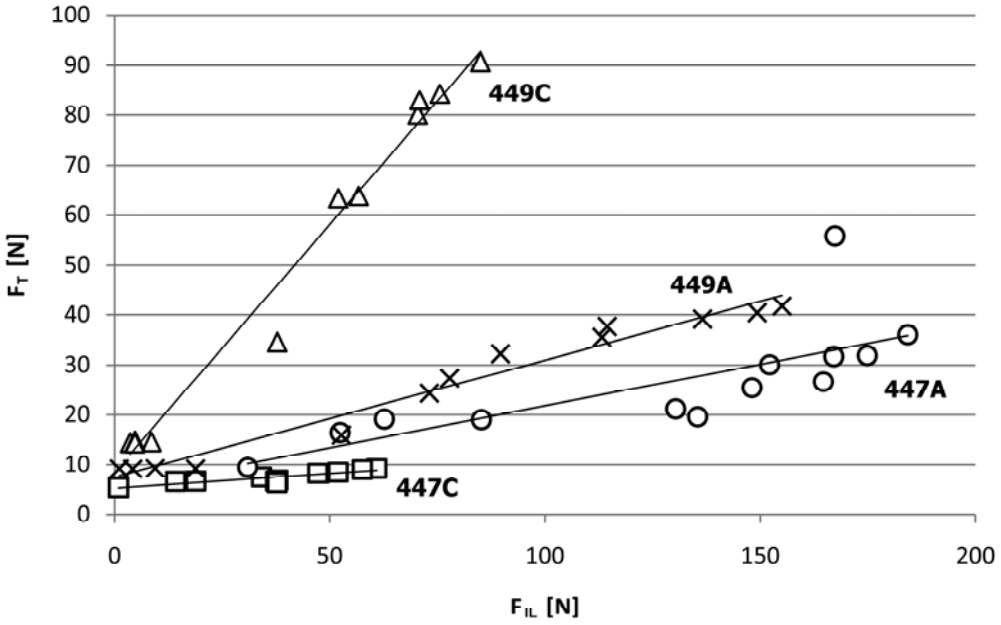

Figure 5. Transverse force F_T acting on the IPM implant versus in-line force F_{IL} of the *Pectoralis major* during the electrical stimulation experiments for the two chronic and two acute implants. The trend lines were obtained with simple linear regression.

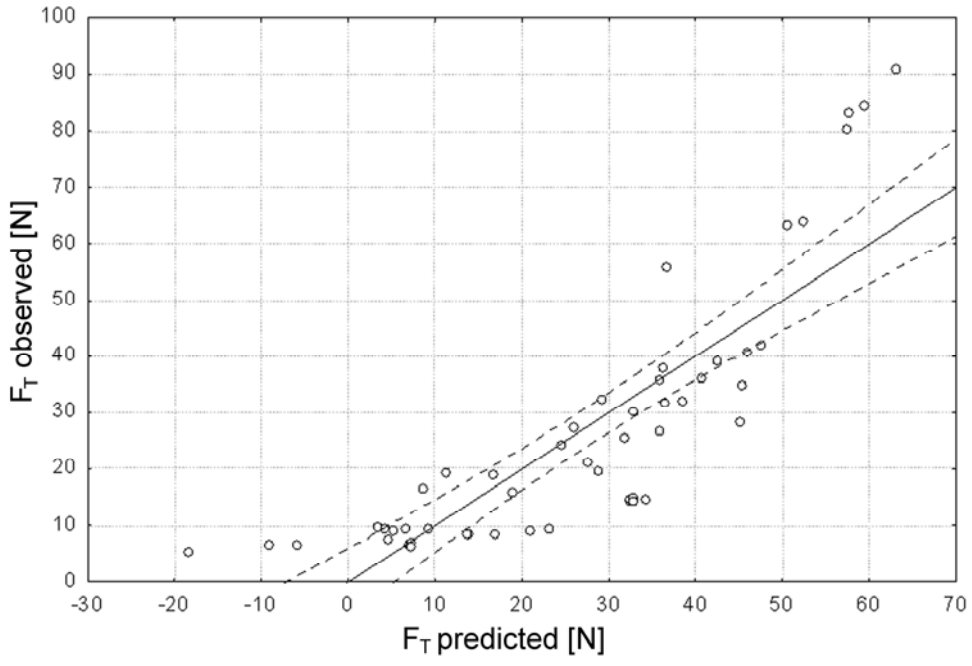

Figure 6. Observed vs. predicted transverse force F_T of the *Pectoralis major* in the baboon. The prediction was obtained from the intra-species correlation equation established (Eq. 4). The dashed lines indicate the 95% confidence interval.